Sagnac effect of excitonic polaritons

Lijuan Gu,[1,*] Hai Huang,[2] and Zizhao Gan[1]

[1]*State Key Laboratory of Mesoscopic Physics, School of Physics, Peking University, Beijing 100871, China*

[2]*Department of Mathematics and Physics, North China Electric Power University, Beijing 102206, China*

(Received 24 August 2010; revised manuscript received 28 April 2011; published 1 August 2011)

We theoretically treat the Sagnac effect of excitonic polaritons in bulk material and microcavity. Using the coupling between the electromagnetic and excitonic waves, the rotational sensitivity per unit area of a Sagnac loop can be tuned from light to exciton behavior by varying frequency. We also discuss the feasibility and the difficulties of the hybrid light-exciton wave Sagnac interferometer. We show that the quasi-two-dimensional microcavity excitonic polariton is a better candidate than the bulk one. Considering the short decoherence time in semiconductors, we suggest using the degenerate four-wave mixing of the microcavity excitonic polaritons to generate two intrinsically coherent conjugate waves.

DOI: 10.1103/PhysRevB.84.075402 PACS number(s): 42.81.Pa, 73.20.Mf, 78.67.−n, 42.65.Hw

I. INTRODUCTION

In 1913, Sagnac demonstrated the feasibility of using a ring interferometer to detect the rotation of a system, in which the interferometer is at rest.[1] The phase difference between two counterpropagating light beams in a closed loop is

$$\Delta\Phi = 4\eta\Omega\cdot\mathbf{A}, \tag{1}$$

where Ω is the angular velocity of the system and $\mathbf{A}$ is the vector of the loop area. The coefficient η is

$$\eta = \eta_p = \frac{\omega}{c^2}, \tag{2}$$

where ω is the frequency of the light and c is the velocity of light in vacuum. Even if the light is propagating in a medium, the coefficient is the same.[2–4] A similar effect occurs in the ring interferometer of matter wave, but the coefficient is[5–8]

$$\eta = \eta_m = \frac{m}{\hbar}, \tag{3}$$

where m is the mass of the particle and $\hbar$ is the reduced Planck constant. The Sagnac phase shift per unit area in a matter-wave device exceeds that of laser-based interferometers by the ratio of $\frac{mc^2}{\hbar\omega}$; taking the visible light and electrons as an example, the ratio is about 10^5.

In order to combine the large loop area in the light system and high rotational sensitivity per unit area in matter wave devices, Zimmer and Fleischhauer have proposed a light-matter wave Sagnac interferometer based on the slow-light propagation in ultracold atomic vapor,[9] in which the light can be coupled to the atomic Raman resonance to form the so-called dark-state polaritons. Following similar ideas, in this paper we discuss the feasibility of the hybrid light-matter wave Sagnac interferometer based on excitonic polaritons in semiconductors, which are quasiparticles coupled by photons and dipole active excitons.[10–12]

The Sagnac effect of the excitonic polaritons can be expressed as follows. In a rotational system, the equations of the electromagnetic wave and the excitonic wave have to take some corrections. We calculate wave equations in a rotational system to first order in $\frac{|\Omega|}{c}$ and, compared with the result in an inertial system, the wave vector of the electromagnetic wave here has an additional term $\delta\mathbf{k} = \eta_p(\mathbf{v}_R\cdot\mathbf{e}_k)\mathbf{e}_k$, where $\mathbf{v}_R = \Omega\times\mathbf{R}$ and $\mathbf{e}_k$ is the unit vector of $\mathbf{k}$; similarly, the wave vector of the excitonic wave has an additional term $\delta\mathbf{k} = \eta_m(\mathbf{v}_R\cdot\mathbf{e}_k)\mathbf{e}_k$, which is the same as the matter wave with an effective mass m. Next, when we consider the coupling between an electromagnetic wave and an excitonic wave, a new type of quasiparticles called polaritons appear. The wave vector of the polariton also has an additional term in the rotational system,

$$\delta k = \eta_{\mathrm{eff},i}(\mathbf{v}_R\cdot\mathbf{e}_k). \tag{4}$$

Here i indicates the energy branches of the polariton (as it will be stated in the following) and $\eta_{\mathrm{eff},i}$ is the effective coefficient. Therefore, the Sagnac effect of the excitonic polariton is

$$\Delta\Phi = 4\eta_{\mathrm{eff},i}\Omega\cdot\mathbf{A}. \tag{5}$$

We hope to obtain a big $\eta_{\mathrm{eff},i}$ to get a high sensitivity and simultaneously we want to have a large photon proportion so that the shot-noise level is low. Therefore, we calculate the coefficient $\eta_{\mathrm{eff},i}$ and the photon proportion of the excitonic polaritons as functions of frequency ω. It appears that when ω approaches to the exciton frequency, $\eta_{\mathrm{eff},i}$ gradually increases from $\frac{\omega}{c^2}$ to $\frac{m}{\hbar}$, while the photon proportion decreases from 1 to 0; here, m is the effective mass of the exciton. Therefore, it is possible to choose a suitable frequency so that the excitonic polariton wave can possess a large value of $\eta_{\mathrm{eff},i}$ and a moderate proportion of photon simultaneously. This is a favorable factor for constructing the Sagnac interferometer based on excitonic polaritons.

Owing to momentum conservation, direct transition from photons to the bulk excitonic polaritons is prohibited. As a result, keeping the phase relations in the bulk hybrid light-exciton interferometer is very difficult. Moreover, the decoherence time of the bulk excitonic polaritons is usually very short, which is another serious problem for the Sagnac interferometer based on bulk excitonic polaritons. A better candidate is the excitonic polaritons in semiconductor microcavity with one or a few quantum wells embedded at the antinodes of its intracavity mode. These are two-dimensional quasiparticles and the direct transition from the external photons to such two-dimensional quasiparticles is possible because momentum conservation in the optical transition needs to be satisfied only in the quantum well plane but

not along the confinement direction. In addition, scattering of the lower branch microcavity excitonic polaritons by phonons is suppressed remarkably in the neighborhood of the origin of the two-dimensional Brillouin zone. Therefore, the decoherence time of the lower branch microcavity excitonic polaritons is much longer than that of the bulk excitonic polaritons. However, even using a high quality semiconductor microcavity, measurement of the decoherence time is shorter than 10 ps, which is also very short.

Therefore, in order to solve this problem, we use the degenerate four-wave mixing (DFWM) of the microcavity excitonic polaritons. Due to the exciton-exciton interaction, third-order nonlinear effects are strengthened remarkably. Many theoretical and experimental works have reported the third-order nonlinear effects of the excitonic polaritons.[13–19] During the DFWM process, two conjugate waves with counterpropagating directions are generated and those two waves are intrinsically coherent. We also demonstrate that the phase difference between the two conjugate wave has a form similar to the Sagnac phase difference obtained from the excitonic polariton. Therefore, we can use this process in our hybrid interferometer.

The paper is organized as follows. In Sec. II, we discuss the Sagnac effect of the bulk excitonic polariton and the difficulties of the Sagnac interferometer based on it. Then the Sagnac effect of microcavity excitonic polaritons and their advantages are discussed in Sec. III. The Sagnac effect for the DFWM of microcavity excitonic polaritons is discussed in Sec. IV. Some brief conclusions are made in Sec. V.

II. SAGNAC EFFECT OF THE EXCITONIC POLARITONS

A. Electromagnetic wave and excitonic wave in a rotational system

In a rotational system, which is not inertial, the Maxwell equations should make some changes. We obtain the Maxwell equations to first order in $\frac{|\Omega|}{c}$; the first pair is

$$\begin{aligned} \nabla\cdot\mathbf{B} &= 0, \\ \nabla\times\mathbf{E} &= -\frac{1}{c}\frac{\partial\mathbf{B}}{\partial t}. \end{aligned} \tag{6}$$

It is the same as in the inertial system and the second pair is

$$\begin{aligned} \nabla\cdot\left(\mathbf{E}-\frac{1}{c}\mathbf{v}_R\times\mathbf{B}\right) &= 4\pi\rho, \\ \nabla\times\left(\mathbf{B}-\frac{1}{c}\mathbf{v}_R\times\mathbf{E}\right) &= \frac{1}{c}\frac{\partial}{\partial t}\left(\mathbf{E}-\frac{1}{c}\mathbf{v}_R\times\mathbf{B}\right)+\frac{4\pi}{c}\mathbf{j}. \end{aligned} \tag{7}$$

Here $\mathbf{E}$ and $\mathbf{B}$ are the electric field and the magnetic field; ρ and $\mathbf{j}$ are the charge density and the electric current density. In dielectric,

$$\begin{aligned} \rho &= -\nabla\cdot\mathbf{P}, \\ \mathbf{j} &= \frac{\partial\mathbf{P}}{\partial t}. \end{aligned} \tag{8}$$

Here $\mathbf{P}$ is the dielectric polarization. Then we have

$$\frac{1}{c^2}\frac{\partial^2\mathbf{E}}{\partial t^2}-\nabla^2\mathbf{E}-2\frac{\mathbf{v}_R}{c}\cdot\nabla\left(\frac{1}{c}\frac{\partial\mathbf{E}}{\partial t}\right)=-\frac{4\pi}{c^2}\frac{\partial^2\mathbf{P}}{\partial t^2}, \tag{9}$$

$$\nabla\cdot(\mathbf{E}+4\pi\mathbf{P})=-\frac{\mathbf{v}_R}{c^2}\cdot\frac{\partial(\mathbf{E}+4\pi\mathbf{P})}{\partial t}. \tag{10}$$

The third term on the left-hand side of Eq. (9) and the right-hand side of Eq. (10) are correction terms that do not exist in inertial systems. In the usual dielectric, if frequency of the electromagnetic field is far away from the exciton resonance frequency, the polarization is linear with the electric field and their relation is local; that is,

$$\mathbf{P}_c=\kappa_c\mathbf{E}. \tag{11}$$

Therefore, Eq. (9) becomes

$$\frac{\epsilon_c}{c^2}\frac{\partial^2\mathbf{E}}{\partial t^2}-\nabla^2\mathbf{E}-2\frac{\mathbf{v}_R}{c}\cdot\nabla\left(\frac{1}{c}\frac{\partial\mathbf{E}}{\partial t}\right)=0. \tag{12}$$

Here $\epsilon_c=1+4\pi\kappa_c$.

Using a quasiclassical approximation, we can write the electric field as

$$\mathbf{E}=A\exp(-j\omega t+\mathbf{k}\cdot\mathbf{r}). \tag{13}$$

Inserting it into Eq. (12),

$$k^2-2\frac{\omega}{c^2}(\mathbf{v}_R\cdot\mathbf{e}_k)k-\frac{\epsilon\omega^2}{c^2}=0, \tag{14}$$

we get

$$k\approx\sqrt{\epsilon}\frac{\omega}{c}+\frac{\omega}{c^2}(\mathbf{v}_R\cdot\mathbf{e}_k). \tag{15}$$

After integrating over the Sagnac loop, we can have Eq. (1) and Eq. (2). The Sagnac effect only results from the additional term $\delta\mathbf{k}=\frac{\omega}{c^2}(\mathbf{v}_R\cdot\mathbf{e}_k)\mathbf{e}_k$, and it has nothing to do with the medium property.

When the frequency of the propagating light in a semiconductor approaches the α-exciton state resonance frequency ω_α, the dipole active exciton contributes to the polarization in the semiconductor. Also, the polarization includes two parts:

$$\mathbf{P}=\mathbf{P}_c+\mathbf{P}_\alpha. \tag{16}$$

Here $\mathbf{P}_c$ is the same as that in Eq. (11). It is contributions from all the other excited states that are far away from resonance; $\mathbf{P}_\alpha$ is a contribution from the resonant α-exciton state. Now Eq. (9) becomes

$$\frac{\epsilon_c}{c^2}\frac{\partial^2\mathbf{E}}{\partial t^2}-\nabla^2\mathbf{E}-2\frac{\mathbf{v}_R}{c}\cdot\nabla\left(\frac{1}{c}\frac{\partial\mathbf{E}}{\partial t}\right)=-\frac{4\pi}{c^2}\frac{\partial^2\mathbf{P}_\alpha}{\partial t^2}. \tag{17}$$

In order to make the discussion specifically, we only consider the Mott-Wannier exciton, which can be regarded as an electron-hole pair and its motion can be divided into two parts. One is the relative motion between the electron and the hole; the eigenvalue of this Hamiltonian determines its resonance frequency ω_α. Another part is the motion of the exciton mass center and the Hamiltonian of this part can be written as

$$H_{M,\alpha}=\hbar\omega_\alpha-\frac{\hbar^2}{2M}\nabla^2. \tag{18}$$

Here M is the total mass of the α exciton. If the exciton interparticle spacing is much larger than its Bohr radius, the excitons can be regarded as bosons and the wave function of the mass center can be regarded as the excitonic wave

function.[20–22] Therefore, we can write that the polarization induced by the α exciton is

$$\mathbf{P}_\alpha = \mathbf{l}_\alpha(\Psi_\alpha + \Psi_\alpha{}^*). \tag{19}$$

Here Ψ_α is the wave equation of the α exciton and $\mathbf{l}_\alpha$ is the matrix element between the ground state and the α-exciton state. Interaction between this polarization and the electric field is $-\mathbf{P}_\alpha \cdot \mathbf{E}$; then we can get the wave equation of the exciton,

$$\frac{\partial^2 \mathbf{P}_\alpha}{\partial t^2} + \left(\frac{H_{M,\alpha}}{\hbar}\right)^2 \mathbf{P}_\alpha - \frac{H_{M,\alpha}}{\hbar}\frac{\mathbf{l}_\alpha \mathbf{l}_\alpha}{\hbar} \cdot \mathbf{E} = 0. \tag{20}$$

Next we consider the exciton wave equation in a rotational system. In that case, the electron-hole Hamiltonian will have extra terms related to the rotational velocity. For the relative motion between electron and hole, the additional term turns out to be $(\Omega \times \mathbf{r}_r) \cdot \mathbf{p}_r$, where $\mathbf{r}_r$ and $\mathbf{p}_r$ are the relative coordinate and momentum of the electron-hole pair, respectively, while for the mass center Hamiltonian, there is an additional term $(\Omega \times \mathbf{r}_M) \cdot \mathbf{p}_M$, where $\mathbf{r}_M$ and $\mathbf{p}_M$ are the mass center coordinate and momentum accordingly. While the term $(\Omega \times \mathbf{r}_r) \cdot \mathbf{p}_r$ only changes the resonance frequency ω_α, the change is so small that we can neglect it. Therefore, we only consider the mass center part and assume the matrix element is isotropic, and Eq. (20) becomes

$$\frac{\partial^2 \mathbf{P}_\alpha}{\partial t^2} + \left(\omega_\alpha - \frac{\hbar}{2M}\nabla^2 + j\mathbf{v}_R \cdot \nabla\right)^2 \mathbf{P}_\alpha - \frac{2l_\alpha^2}{\hbar}\left(\omega_\alpha - \frac{\hbar}{2M}\nabla^2 + j\mathbf{v}_R \cdot \nabla\right)\mathbf{E} = 0. \tag{21}$$

In the extreme case $\mathbf{E} = 0$, using a quasiclassical approximation, we get $k = \sqrt{\frac{2M(\omega-\omega_\alpha)}{\hbar}} + \frac{M}{\hbar}(\mathbf{v}_R \cdot \mathbf{e}_k)$; that is, Sagnac behavior of the exciton wave is the same as a matter wave with its effective mass M.

Therefore, we have obtained the coupling wave equations between the light wave and the exciton wave—Eq. (12) and Eq. (21). In inertial system $\Omega = 0$, by solving these two equations, we get two branches of the excitonic polaritons with different eigenenergies; in the following, we consider the rotational system and will use these coupling wave equations to discuss the Sagnac effect of the excitonic polaritons.

B. Excitonic polariton and its Sagnac effect

Again, we use the quasiclassical approximation,

$$(E, P_\alpha) = (E_k, P_{\alpha,k}) \exp(-j\omega t + j\mathbf{k} \cdot \mathbf{r}). \tag{22}$$

Then, Eq. (12) and Eq. (21) become

$$\left[k^2 - \epsilon_c \frac{\omega^2}{c^2} - 2\frac{\omega}{c^2}(\mathbf{v}_R \cdot \mathbf{e}_k)k\right] E_k - \frac{4\pi\omega^2}{c^2} P_{\alpha,k} = 0, \tag{23}$$

$$\{[\omega_{\alpha,k} - (\mathbf{v}_R \cdot \mathbf{e}_k)k]^2 - \omega^2\} P_{\alpha,k} - \frac{\epsilon_c \omega_{\alpha,k}}{2\pi}\Delta_{\mathrm{LT}} E_k = 0, \tag{24}$$

where $\omega_{\alpha,k} = \omega_\alpha + \frac{\hbar k^2}{2M}$ and $\Delta_{\mathrm{LT}} = \frac{4\pi l_\alpha^2}{\hbar \epsilon_c}$. It is reasonable to take the approximation

$$\omega_{\alpha,k} - (\mathbf{v}_R \cdot \mathbf{e}_k)k + \omega \approx 2\omega_{\alpha,k}. \tag{25}$$

Then the coupling wave equations become

$$\begin{bmatrix} Q(k) - 2\eta_p(\mathbf{v}_R \cdot \mathbf{e}_k)k & -\frac{4\pi}{c^2}\omega^2 \\ -\frac{\epsilon_c}{4\pi}\frac{2M\Delta_{\mathrm{LT}}}{\hbar} & R(k) - 2\eta_M(\mathbf{v}_R \cdot \mathbf{e}_k)k \end{bmatrix} \begin{bmatrix} E_k \\ P_{\alpha,k} \end{bmatrix} = 0. \tag{26}$$

In deriving the above result, we introduced the following notations:

$$k_c^2 = \epsilon_c \frac{\omega^2}{c^2}, \eta_p = \frac{\omega}{c^2}, \quad \eta_M = \frac{M}{\hbar},$$
$$Q(k) = k^2 - {k_c}^2, R(k) = k^2 + \frac{2M}{\hbar}(\omega_\alpha - \omega). \tag{27}$$

From this equation, we can obtain k as a function of ω, that is, the dispersion relation of the excitonic polariton wave. We solve this equation by expanding k in powers of $(\frac{v_R}{c})$; the zeroth-order equation is

$$Q(k)R(k) = \frac{2M}{\hbar}{k_c}^2 \Delta_{\mathrm{LT}}. \tag{28}$$

There are two branches of solutions for Eq. (28),

$${k_{L,U}}^2 = \frac{1}{2}\left[{k_c}^2 - \frac{2M}{\hbar}(\omega_\alpha - \omega)\right] \pm \sqrt{\left[{k_c}^2 + \frac{2M}{\hbar}(\omega_\alpha - \omega)\right]^2 + \frac{8M}{\hbar}{k_c}^2 \Delta_{\mathrm{LT}}}, \tag{29}$$

where "+"corresponds to the dispersion of the lower branch of the excitonic polaritons (LPB), and "−"corresponds to the upper branch of the excitonic polaritons (UPB).[11,12]

The first-order solution is

$$\delta k_i = \frac{\eta_p + D_i \eta_M}{1 + D_i}(\mathbf{v}_R \cdot \mathbf{e}_k). \tag{30}$$

Here $i = L$ or U and

$$D_i(\omega) = \frac{\hbar}{2M}\frac{Q^2(k_i)}{{k_c}^2 \Delta_{\mathrm{LT}}}, \tag{31}$$

Defining the effective coefficient as

$$\eta_{\mathrm{eff},i} = \frac{\eta_p + D_i(\omega)\eta_M}{1 + D_i(\omega)}, \tag{32}$$

we have the phase difference between the clockwise and counterclockwise wave as

$$\Delta\Phi = 2\oint \delta\mathbf{k}_i \cdot d\mathbf{l} = 4\eta_{\mathrm{eff},i}\,\Omega \cdot \mathbf{A}. \tag{33}$$

Therefore, the effective Sagnac coefficient of the i-branch excitonic polariton with frequency ω is $\eta_{\mathrm{eff},i}$.

In order to build a hybrid Sagnac interferometer, we also have to guarantee that the photon flux is large enough to get a lower shot-noise level. Now we calculate the photon proportion of the excitonic polariton. The method is that, first, we transform the equations of E_k and $P_{\alpha,k}$ into equations of the amplitude of the photon wave A_k and the amplitude of exciton wave $F_{\alpha,k}$. Second, we write the annihilation operator of the i-branch excitonic polariton as $c_{\mathrm{ph},i}a_k + c_{\mathrm{ex},i}b_{\alpha,k}$; here,

a_k and $b_{\alpha,k}$ are the annihilation operators of photon and the α exciton, respectively. Finally, we get the coefficient

$$c_{\mathrm{ph},i} = j\frac{\omega^2\sqrt{2\Delta_{\mathrm{LT}}/\omega_{k,i}}}{\sqrt{(\omega^2-{\omega_{k,i}}^2)^2+\omega^4(2\Delta_{\mathrm{LT}}/\omega_{k,i})}},$$
$$c_{\mathrm{ex},i} = \frac{\omega^2-{\omega_{k,i}}^2}{\sqrt{(\omega^2-{\omega_{k,i}}^2)^2+\omega^4(2\Delta_{\mathrm{LT}}/\omega_{k,i})}}, \quad (34)$$

where $\omega_{k,i} = \frac{ck_i}{\sqrt{\epsilon_c}}$.

We use the following notations for simplification and change all the quantities into dimensionless ones:

$$k_{c,\alpha} = \frac{\sqrt{\epsilon_c}}{c}\omega_\alpha, \quad x = \frac{\omega}{\omega_\alpha}, \quad q = \frac{k}{k_{c,\alpha}}, \quad \delta_{\mathrm{LT}} = \frac{\Delta_{\mathrm{LT}}}{\omega_\alpha},$$
$$r_\alpha = \frac{\hbar\omega_\alpha}{2Mc^2}, \quad A = \frac{1}{\epsilon_c r_\alpha}, \quad B = 4A\delta_{\mathrm{LT}}. \quad (35)$$

Using these notations, Eqs. (29), (31), and (34) can be rewritten as

$$q_i^2 = \frac{1}{2}[x^2 - A(1-x)] \pm \sqrt{[x^2+A(1-x)]^2 + Bx^2},$$
$$D_i = \frac{4}{B}\frac{({q_i}^2-x^2)^2}{x^2}, \quad (36)$$
$$c_{\mathrm{ph},i} = j\sqrt{\frac{2\delta_{\mathrm{LT}}(x^4/q_i)}{({q_i}^2-x^2)^2+2\delta_{\mathrm{LT}}(x^4/q_i)}},$$
$$c_{\mathrm{ex},i} = \sqrt{\frac{x^2-{q_i}^2}{({q_i}^2-x^2)^2+2\delta_{\mathrm{LT}}(x^4/q_i)}},$$

and $\eta_p = \frac{\omega_\alpha}{c^2}x$, $\frac{\eta_p}{\eta_M} = 2r_\alpha x$.

C. An example: Excitonic polaritons in GaN

GaN is a kind of III-V compound; it has large exciton binding energy (≈50 meV) and oscillation strength, and it had been demonstrated that excitons in it are stable at room temperature. AAlso, due to the progress of material technology in the past few years, lasing and Bose-Einstein condensation of the excitonic polariton have been demonstrated in the GaN cavity at room temperature. Therefore, we choose it as an example to calculate the Sagnac effect of bulk excitonic polaritons. The parameters of the A exciton of GaN are[23,24]

$$\hbar\omega_\alpha = 3.487\ \mathrm{eV}, \Delta_{\mathrm{LT}} = 3.0\ \mathrm{meV},$$
$$M = 1.3m_e, \epsilon_c = 8.75. \quad (37)$$

Because the upper polariton branch suffers more serious scattering than the lower polariton branch, it has a much shorter decoherence time and shorter radiative lifetime. As a result, we mainly discuss the results of the lower polariton branch. The dispersion relations are shown in Fig. 1. We can find that the dispersion curve $q_L(x)$ deviates from the dispersion curve of photon $q_p(x) = x$ remarkably from the beginning point $x = 0.990$, and then gradually approaches the dispersion curve of exciton $q_{\mathrm{ex}}(x) = \sqrt{A(x-1)}$. Also, at large wave vectors, dispersion of the LPB and UPB converge to the exciton and photon dispersions, respectively.

Figure 2 shows the effective coefficient $\eta_{\mathrm{eff},L}$ as a function of x. At the beginning, $\eta_{\mathrm{eff},L}(x)$ is close to $\eta_p = \frac{\omega_\alpha}{c^2}x$. Then it increases very quickly within a narrow interval around

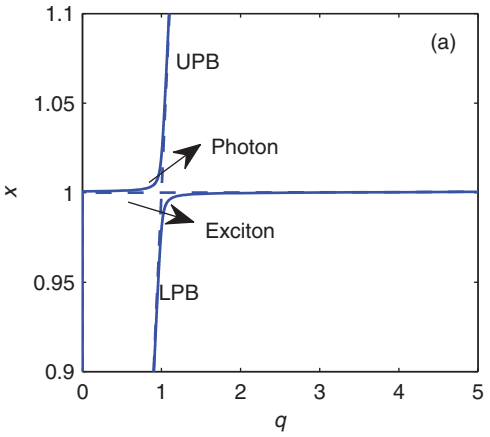

FIG. 1. (Color online) Dispersion curves of the excitonic polaritons (solid line). LPB represents the lower polariton branch and UPB represents the upper polariton branch. The dashed lines are the dispersion curves of the photons and excitons, respectively.

$x = 1$. As is shown in Fig. 2, at $x = 0.990$, $\eta_{\mathrm{eff},L}$ increases to 2.1884 s m^{-2}, which is approximatedly 35 times the value of η_p, while at $x = 0.999$, $\eta_{\mathrm{eff},L}(x)$ rises to 197.5422 s m^{-2}, which is 3700 times of the value of η_p. Finally, $\eta_{\mathrm{eff},L}(x)$ approaches $\eta_M = \frac{M}{\hbar} \approx 1.1\times10^4$ s m^{-2}. In Fig. 3, the proportion of the photon is shown as a function of x. We can find that the value of $n_{\mathrm{ph},L}(x)$ begins at less than 1 and then drops very quickly in the small interval next to $x = 1$. As it has been shown in this figure, at $x = 0.990$, $n_{\mathrm{ph},L} \approx 0.19$, and at $x = 0.995$, $n_{\mathrm{ph},L}$ drops to 0.002.

In order to evaluate the influence of the material parameters on these results, we make the calculation using the same parameters with Eq. (37), except that the effective mass of the exciton $M = 13m_e$; the values of $\eta_{\mathrm{eff},L}(x)$ and $n_{\mathrm{ph},L}(x)$ are shown in Figs. 4 and 5, respectively. It is clear that the behaviors are similar to the case with $M = 1.3m_e$.

Therefore, it is evident that at suitable x, the excitonic polariton wave can provide us with a large value of $\eta_{\mathrm{eff},L}(x)$ and a moderate value of $n_{\mathrm{ph},L}(x)$ simultaneously. If we construct a hybrid light-exciton wave interferometer just like Fig. 6,

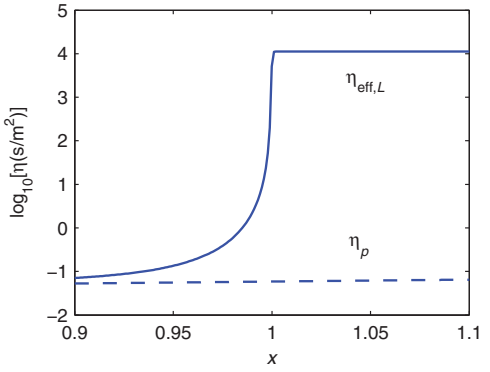

FIG. 2. (Color online) Effective Sagnac coefficient of bulk GaN excitonic polaritons (solid line) and Sagnac coefficient of the photons (dashed line); $M = 1.3m_e$.

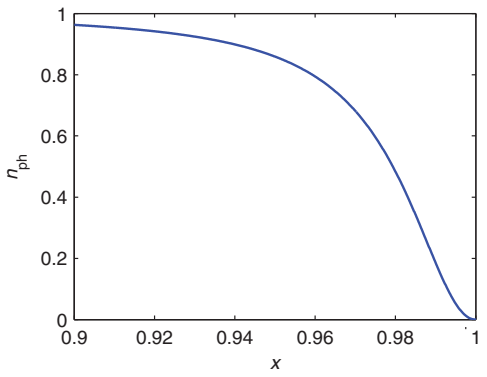

FIG. 3. (Color online) Photon proportion of bulk GaN excitonic polaritons; $M = 1.3m_e$.

the phase difference between the two counterpropagating beams is

$$\Delta\Phi = 4\frac{l_1\eta_p + l_2\eta_{\text{eff}}}{l_1 + l_2}\Omega l_1 l_2. \tag{38}$$

If light frequency ω is close to the resonance frequency of the α-exciton ω_α, the sensitivity of the hybrid interferometer can be enhanced by a factor of $\frac{1}{l_1+l_2}(l_1 + l_2\frac{\eta_{\text{eff}}}{\eta_p})$ than the common laser interferometer.

D. Some intrinsical difficulties of the bulk excitonic polariton

Nevertheless, there are some intrinsical difficulties for such a hybrid interferometer. First of all, conservation of energy and momentum prohibits direct transition from photons to the bulk excitonic polaritons unless some higher-order processes occur, for example, the scattering of the photons or excitons by interface, phonons, or defects in the crystal. However, these higher-order processes are complicated and may destroy the phase relations of these waves, so Eq. (38) is not correct in this case and has to make some corrections. It is a very complicated problem to calculate, so keeping a stable phase relation in such an interferometer is very difficult.

The second difficulty is that the decoherence time of the bulk excitonic polariton wave is usually very short, much shorter than 1 ps at room temperature. The dominant decoherent processes of the excitonic polaritons are the scattering

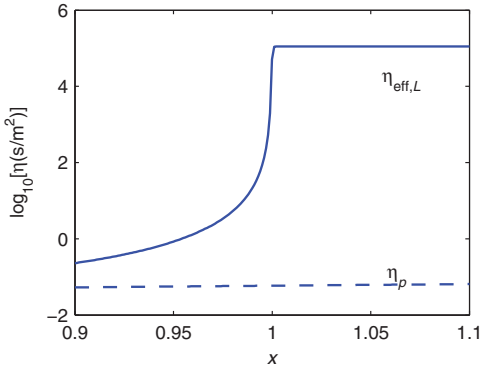

FIG. 4. (Color online) Effective Sagnac coefficient of bulk GaN excitonic polaritons (solid line) and Sagnac coefficient of the photons (dashed line); $M = 13m_e$.

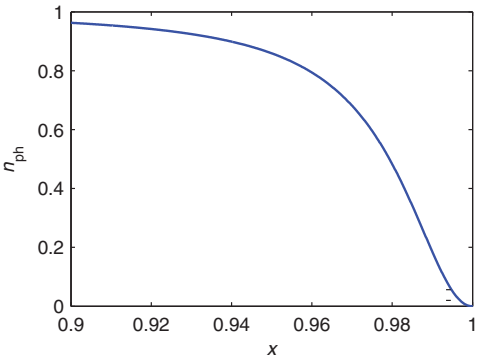

FIG. 5. (Color online) Photon proportion of bulk GaN excitonic polaritons; $M = 13m_e$.

processes of the excitons by other excitons, photons, or various defects in the crystal. A phenomenological description of the decoherence of excitons can be given by inserting a relaxation term into Eq. (20). Then it becomes

$$\frac{\partial^2\mathbf{P}_\alpha}{\partial t^2} + \left(\frac{H_{M,\alpha} - \mathbf{v}_R\cdot\mathbf{p}}{\hbar}\right)^2\mathbf{P}_\alpha + \Gamma_\alpha\frac{\partial\mathbf{P}_\alpha}{\partial t} - 2\frac{\mathbf{l}_\alpha\mathbf{l}_\alpha}{\hbar}\cdot\left(\frac{H_{M,\alpha} - \mathbf{v}_R\cdot\mathbf{p}}{\hbar}\right)\mathbf{E} = 0. \tag{39}$$

Here the coefficient ${\Gamma_\alpha}^{-1}$ can be understood as the decoherence time of the excitonic wave.

The decoherent processes also occur in light waves; similarly, the effects of these processes can be described by inserting an extra imaginary part in the dielectric constant. In that case, Eq. (12) changes into

$$\frac{\epsilon_c + j\gamma_c}{c^2}\frac{\partial^2\mathbf{E}}{\partial t^2} - \nabla^2\mathbf{E} - 2\frac{\mathbf{v}_R}{c^2}\cdot\nabla\left(\frac{1}{c}\frac{\partial\mathbf{E}}{\partial t}\right) = -\frac{4\pi}{c^2}\frac{\partial^2\mathbf{P}_\alpha}{\partial t^2}. \tag{40}$$

In the quasiclassical approximation, Eqs. (39) and (40) become

$$\left[k^2 - \epsilon_c\frac{\omega^2}{c^2} - 2\frac{\omega}{c^2}(\mathbf{v}_R\cdot\mathbf{e}_k) - j\gamma_c\frac{\omega^2}{c^2}\right]E_k - \frac{4\pi\omega^2}{c^2}P_{\alpha,k} = 0, \tag{41}$$

$$\{[(\omega_{\alpha,k} - \mathbf{v}_R\cdot\mathbf{e}_k)k]^2 - \omega^2 - j\Gamma_\alpha\omega\}P_{\alpha,k} - \frac{\epsilon_c\omega_{\alpha,k}}{2\pi}\Delta_{\text{LT}}E_k = 0. \tag{42}$$

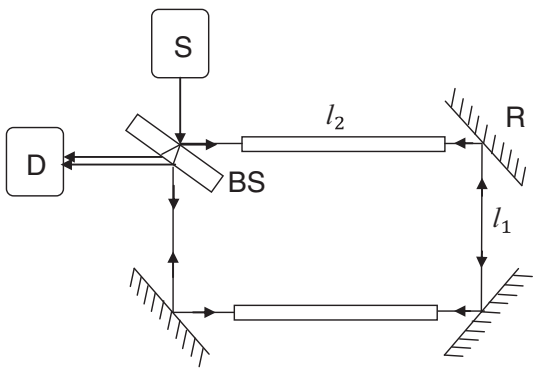

FIG. 6. Schematic of the hybrid light-exciton wave interferometer. S: laser source; D: detector; BS: beam splitter; R: reflect mirror.

Using the same method in Sec. II B to deal with these imaginary terms, we can obtain the first-order corrections for k_i:

$$\delta k_i = \eta_{\mathrm{eff},i}(\mathbf{v}_R \cdot \mathbf{e}_k) + j\frac{\eta_p \omega \gamma_c + D_i \eta_M \Gamma_\alpha}{2k_i(1+D_i)}. \tag{43}$$

When $\eta_{\mathrm{eff},i} \gg \eta_p$, Eq. (43) changes into

$$\delta k_i \approx \eta_{\mathrm{eff},i}\left[(\mathbf{v}_R \cdot \mathbf{e}_k) + j\frac{\Gamma_\alpha}{2k_i}\right]. \tag{44}$$

We can find that the sensitivity of the Sagnac interferometer based on the excitonic polariton wave is limited to $\frac{l_2}{l_1+l_2}\frac{\Gamma_\alpha}{2k_i l_1}$. As the decoherent time of excitons is approximately 1 ps or shorter, it really is a serious difficulty for such a Sagnac interferometer.

III. SAGNAC EFFECT OF THE MICROCAVITY EXCITONIC POLARITONS

A. Excitonic polaritons in microcavity and its Sagnac effect

A typical semiconductor microcavity consists of a pair of distributed Bragg reflectors with one or several quantum wells (QWs) embedded at the antinodes of the intracavity light field.[25–27] When the exciton resonance energy coincides with that of a cavity eigenmode, they couple with each other and lead to the generation of excitonic polaritons. As the excitonic polariton is in quasi-two-dimensional propagating mode, momentum conservation needs only to be satisfied in the QW plane but not the confinement direction. This is one reason why we choose the microcavity excitonic polariton rather than the bulk system.

The propagation equation of the excitonic polariton in the cavity is similar to Eq. (12):

$$\frac{\epsilon_c}{c^2}\frac{\partial^2 \mathbf{E}_{2\mathrm{D}}}{\partial t^2} + \left(k_0^2 - \nabla_{2\mathrm{D}}^2\right)\mathbf{E}_{2\mathrm{D}} - \frac{2}{c^2}(\mathbf{v}_R \cdot \nabla_{2\mathrm{D}})\frac{\partial \mathbf{E}_{2\mathrm{D}}}{\partial t} = -\frac{4\pi}{c^2}\xi\frac{\partial^2 \mathbf{P}_{\alpha,2\mathrm{D}}}{\partial t^2}. \tag{45}$$

Here the electric field $\mathbf{E}_{2\mathrm{D}} = \mathbf{e}_{2\mathrm{D}}\phi_0(z)E_{2\mathrm{D}}(x,y,t)$ is propagating in the x-y plane, $\phi_0(z)$ is the longitudinal component of the cavity mode function, $\nabla_{2\mathrm{D}} = (\frac{\partial}{\partial x}, \frac{\partial}{\partial y}, 0)$, k_0 is the longitudinal wave vector, and $\mathbf{e}_{2\mathrm{D}}$ is the polarization direction of the wave. Therefore, the cavity mode can be written as $\mathbf{e}_{2\mathrm{D}}E_A\phi_0(z)\exp[j(k_x x + k_y y) - j\omega_{0,k}t]$ and its frequency as $\omega_{0,k} = \sqrt{\frac{c^2}{\epsilon_c}(k_x^2 + k_y^2 + k_0^2)}$.

In Eq. (45), $\mathbf{P}_{\alpha,2\mathrm{D}}$ is the QW α-exciton polarization; it can be written as $f_\alpha(z)F_\alpha(x,y,t)$. The quasi-two-dimensional propagation function of the exciton is similar to Eq. (20):

$$\frac{\partial^2 \mathbf{P}_{\alpha,2\mathrm{D}}}{\partial t^2} + \left(\frac{H_{\mathrm{ex}}}{\hbar}\right)^2 \mathbf{P}_{\alpha,2\mathrm{D}} - 2\xi\frac{H_{\mathrm{ex}}}{\hbar}\frac{\mathbf{l}_\alpha \mathbf{l}_\alpha}{\hbar} \cdot \mathbf{E}_{2\mathrm{D}} = 0. \tag{46}$$

Here $H_{\mathrm{ex}} = \hbar\omega_\alpha - \frac{\hbar^2}{2M}\nabla_{2\mathrm{D}}^2 + j\hbar\mathbf{v}_R \cdot \nabla_{2\mathrm{D}}$, $\hbar\omega_\alpha$ is the energy of the α exciton, and the parameter $\xi = \int f_\alpha(z)\phi_0(z)dz$. If we introduce $\mathbf{P}_{2\mathrm{D}} = \xi\mathbf{P}_{\alpha,2\mathrm{D}}$ and suppose the dipoles $\mathbf{l}_\alpha$ are isotropic, then with $\Delta_{\mathrm{LT}} = \frac{4\pi(\xi\mathbf{l}_\alpha)^2}{\hbar\epsilon_c}$, Eqs. (45) and (46) can be transformed into

$$\frac{\epsilon_c}{c^2}\frac{\partial^2 \mathbf{E}_{2\mathrm{D}}}{\partial t^2} + \left(k_0{}^2 - \nabla_{2\mathrm{D}}^2\right)\mathbf{E}_{2\mathrm{D}} - \frac{2}{c^2}(\mathbf{v}_R \cdot \nabla_{2\mathrm{D}})\frac{\partial \mathbf{E}_{2\mathrm{D}}}{\partial t} = -\frac{4\pi}{c^2}\frac{\partial^2 \mathbf{P}_{2\mathrm{D}}}{\partial t^2}, \tag{47}$$

$$\frac{\partial^2 \mathbf{P}_{2\mathrm{D}}}{\partial t^2} + \left(\omega_\alpha - \frac{\hbar}{2M}\nabla_{2\mathrm{D}}^2 + j\mathbf{v}_R \cdot \nabla_{2\mathrm{D}}\right)^2 \mathbf{P}_{2\mathrm{D}} - \frac{\epsilon_c \Delta_{\mathrm{LT}}}{2\pi}\left(\omega_\alpha - \frac{\hbar}{2M}\nabla_{2\mathrm{D}}^2 + j\mathbf{v}_R \cdot \nabla\right)\mathbf{E}_{2\mathrm{D}} = 0. \tag{48}$$

Analogous to the calculations in the preceding section, we can obtain

$$k_{L,U}{}^2 = \frac{1}{2}\left[k_d{}^2 - \frac{2M}{\hbar}(\omega_\alpha - \omega)\right] \pm \sqrt{\left[k_d{}^2 + \frac{2M}{\hbar}(\omega_\alpha - \omega)\right]^2 + \frac{8M}{\hbar}k_c{}^2\Delta_{\mathrm{LT}}}. \tag{49}$$

Here $k_c^2 = \epsilon_c\frac{\omega^2}{c^2}$, $k_d^2 = k_c^2 - k_0^2$, and L and U are labeled as the lower and upper branches of the microcavity excitonic polaritons.

Then we get the first-order approximation of the wave vector of the microcavity excitonic polaritons,

$$\delta k_{\mathrm{eff},i} = \eta_{\mathrm{eff},i}(\mathbf{v}_R \cdot \mathbf{e}_k). \tag{50}$$

Here

$$\eta_{\mathrm{eff},i} = \frac{\eta_p + D_i(\omega)\eta_M}{1 + D_i(\omega)}, \quad D_i(\omega) = \frac{\hbar}{2M}\frac{Q_d^2(k_i)}{k_c{}^2\Delta_{\mathrm{LT}}}, \quad Q_d(k) = k^2 - k_d{}^2. \tag{51}$$

We can further simplify the above results that

$$q_{L,U}^2 = \frac{1}{2}\left[x_d^2 - A(1-x)\right] \pm \sqrt{\left[x_d^2 + A(1-x)\right]^2 + Bx^2},$$

$$c_{\mathrm{ph},i} = j\sqrt{\frac{2\delta_{\mathrm{LT}}x^4/\sqrt{q_i^2 + x_0^2}}{\left(q_i^2 - x_d^2\right)^2 + 2\delta_{\mathrm{LT}}x^4/\sqrt{q_i^2 + x_0^2}}}. \tag{52}$$

Here, except for the parameters $x_d^2 = x^2 - x_0^2$ and $x_0 = \frac{ck_0}{\omega_\alpha\sqrt{\epsilon_c}}$, the other parameters have all been defined in the previous section.

B. An example: Microcavity GaN excitonic polaritons

In order to show the properties of microcavity excitonic polaritons, we use the GaN quantum wells embedded in a microcavity as an example. If we ignore the difference between the parameters of the bulk exciton and QW exciton of GaN and also ignore the dielectric constant difference between GaN and the medium in the cavity, then we can calculate the dispersion curves of the lower and upper branch using Eq. (52).

The calculation results are plotted in Fig. 7. It is very hard to illustrate $q_L(x)$ and $q_U(x)$ simultaneously in one figure because, compared with q_L in the region $x \in [0.9, 1.1]$, $q_U(x)$ increases very quickly, but its value is very small. What we are concerned about and going to use is the LPB, so in Fig. 7 (a),

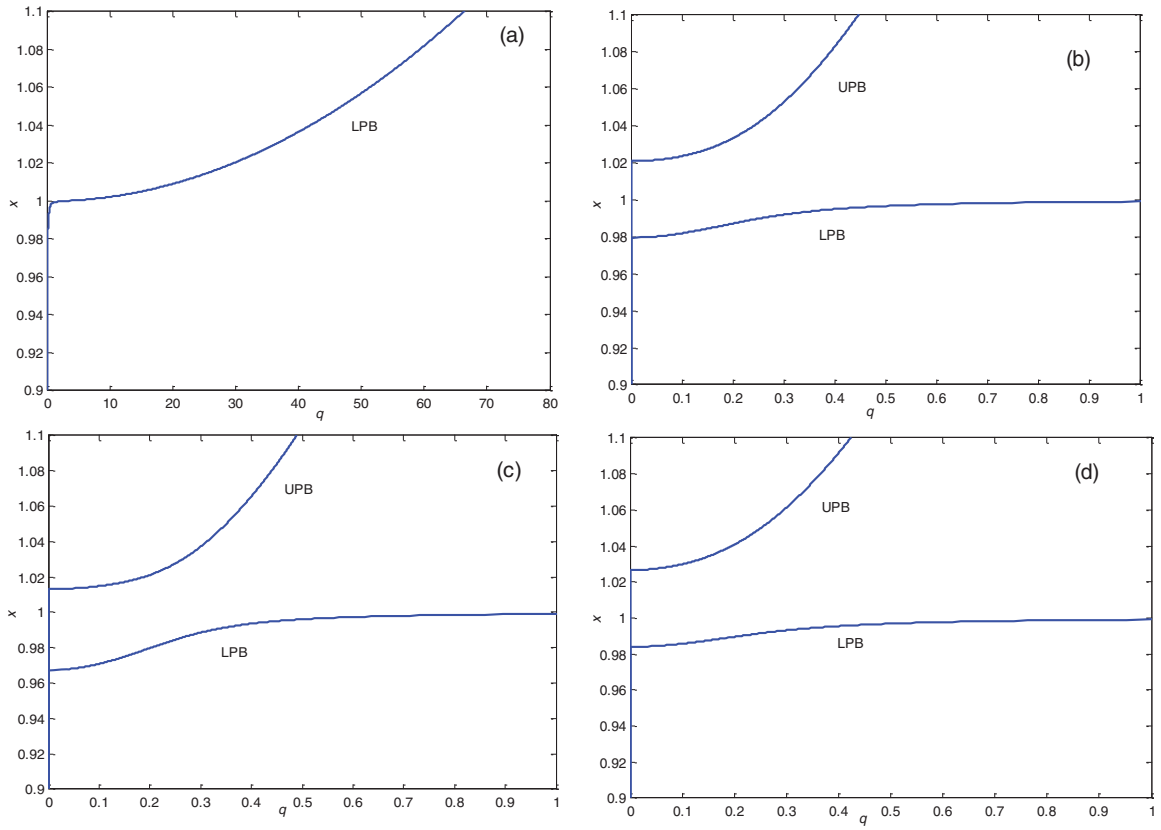

FIG. 7. (Color online) Dispersion curves: (a) the lower polariton branch (LPB) for $x_0 = 1.00$; (b) the upper polariton branch (UPB) and LPB for $x_0 = 1.00$; (c) same as (b) but with $x_0 = 0.98$; (d) same as (b) but with $x_0 = 1.01$.

we show the dispersion curve of the LPB and, in Fig. 7 (b), we illustrate the UPB and LPB simultaneously in the small region $0 < q < 1$. We notice that there is a "pit"around $q = 0$ in the LPB; it acts like the dispersion of the 2D quasiparticle with a very small effective mass. However, in the following, when it approaches $x = 1$, its behavior becomes nonparabolic. It is well known that such a region possesses the so-called bottleneck effect and the scattering by phonons is strongly depressed, so the decoherence time is much longer for the excitonic polaritons in this region.[28,29] In Fig. 7(b), we have $x_0 = 1.00$, while in Figs. 7(c) and 7(d), we have $x_0 = 0.98$ and $x_0 = 1.01$, respectively. The three figures show similar properties, except that the pit depths are different. The depth is deeper at $x_0 = 0.98$ than in the case that $x_0 = 1.00$ and $x_0 = 1.01$.

The effective Sagnac coefficient $\eta_{\mathrm{eff},L}$ and the proportion of photon $n_{\mathrm{ph},L}$ as functions of x are illustrated in Figs. 8 and 9. It is also clear that, at suitable frequency, the microcavity excitonic polaritons can provide us with large values of $\eta_{\mathrm{eff},L}$ and moderate values of $n_{\mathrm{ph},L}$ simultaneously.

The major advantage of the microcavity excitonic polaritons is that momentum conservation in an optical transition needs only to be satisfied in the QW plane but not along the confinement direction. The excitons in a QW couple to light with the same in-plane wave number $k_{\parallel}$ and arbitrary transverse number $k_{\perp}$. Therefore, QWs microcavity is more optically accessible than bulk materials and the first difficulty discussed in Sec. II can be solved in microcavity.

The second difficulty discussed in Sec. II can also be improved in microcavity. In the bottleneck region, scattering of the polaritons by phonons is strongly depressed.[28,29] As a result, the excitonic polaritons in this region have longer decoherence time (some experimental works estimate it as about 10 ps). Nevertheless, it is also too short and, in order to obtain very high sensitivity, we suggest the degenerate four-wave mixing of the microcavity excitonic polariton as a better method.

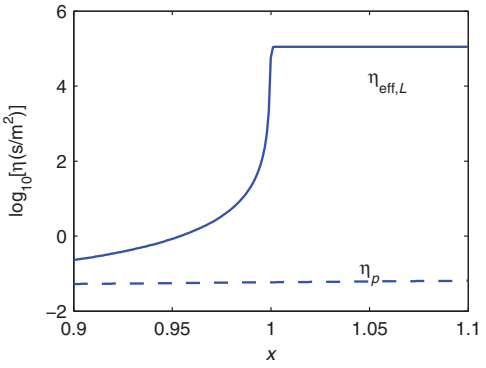

FIG. 8. (Color online) Effective Sagnac coefficient of microcavity GaN excitonic polaritons (solid line) and Sagnac coefficient of the photons (dashed line).

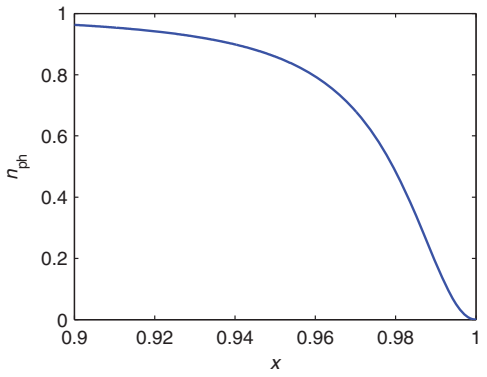

FIG. 9. (Color online) Photon proportion of microcavity GaN excitonic polaritons.

IV. SAGNAC EFFECT IN THE FOUR-WAVE MIXING PROCESS OF MICROCAVITY POLARITON

Due to the excitonic component of the excitonic polaritons and strong confinement in the microcavity, the excitonic polaritons can have strong nonlinear interactions. The third-order nonlinear effects of the microcavity excitonic polaritons, like parametric amplification and degenerate four-wave mixing (DFWM), had been demonstrated in experiments and discussed by theoretical works.[13–15] Among those nonlinear interactions, DWFM is rather important, because it can generate two conjugate waves with opposite directions and these two waves are intrinsically correlative.[16–19] If we can prove that the two conjugate waves can provide us with the Sagnac phase information, they can be used to overcome the problem caused by the short decoherence time of the excitonic polariton. Therefore, in this section, we make a theoretical description of the Sagnac effect of these two conjugate waves and prove that their phase difference is analog with the one we get from the usual Sagnac effect.

A. Nonlinear interaction between the excitonic polaritons

The exciton-exciton interaction in the inertial system can be described by (see Fig. 10)

$$H_{\text{int}} = \sum_{12,34} \left(V_{12,34} b_{\mathbf{k}_1}{}^{\dagger} b_{\mathbf{k}_2}{}^{\dagger} b_{\mathbf{k}_3} b_{\mathbf{k}_4} + \text{c.c.}\right) \delta(\mathbf{k}_1 + \mathbf{k}_2 - \mathbf{k}_3 - \mathbf{k}_4). \tag{53}$$

Here $b_{\mathbf{k}_i}$ and $b_{\mathbf{k}_i}{}^{\dagger}$ are the annihilation and creation operators of the exciton with wave vector $\mathbf{k}_i$.[13,14] Then taking this

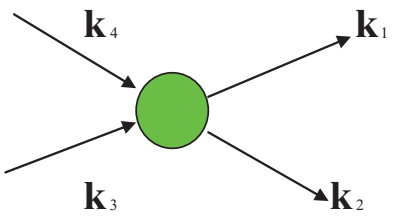

FIG. 10. (Color online) Exciton-exciton interaction in which two excitons $\mathbf{k}_3$ and $\mathbf{k}_4$ are scattered into $\mathbf{k}_1$ and $\mathbf{k}_2$.

interaction into account, the polarization equation of the excitonic wave with wave vector $\mathbf{k}_i$ is similar to Eq. (20), but with an extra term on the right-hand side of the equation,

$$\frac{\partial^2 P_i}{\partial t^2} + \left(\frac{H_M}{\hbar}\right)^2 P_i - \frac{2H_M}{\hbar}\frac{\mathbf{l}_\alpha \mathbf{l}_\alpha}{\hbar} E_i = -2\frac{H_M}{\hbar}\frac{V_{12,34}}{{l_\alpha}^2}\prod_{j\neq i} P_j. \tag{54}$$

In this equation, $i, j = 1,2,3,4$. $\mathbf{P}_i$ is the exciton-induced polarization and H_M is the Hamiltonian of the exciton mass center in an inertial system. We can find that the left-hand side of this equation is the propagation of $\mathbf{P}_i$ and the right-hand side is to describe the creation of $\mathbf{P}_i$ by a third-order nonlinear effect. If we neglect photon-exciton and photon-photon nonlinear interactions, the coupled equations of the exciton and light wave now become

$$\begin{aligned} &\left(-\nabla^2 - \epsilon_c \frac{\omega_i^2}{c^2}\right) E_i - \frac{4\pi\omega_i^2}{c^2} P_i = 0, \\ &\left[-\nabla^2 + \frac{2M}{\hbar}(\omega_\alpha - \omega_i)\right] P_i \\ &- \frac{\epsilon_c}{4\pi}\frac{2M\Delta_{\text{LT}}}{\hbar} E_i = -\frac{2M}{\hbar}\frac{V_{12,34}}{l_\alpha^2}\prod_{j\neq i} P_j. \end{aligned} \tag{55}$$

As we have discussed in Sec. III, if we ignore the nonlinear term, the homogeneous part of Eq. (55) has two branches of solutions corresponding to the lower and upper polariton branch. We combine the electric field and the polarization into a matrix and normalize it; that is,

$$F_{i,\mu} = \begin{pmatrix} E_{i,\mu} \\ P_{i,\mu} \end{pmatrix} = f_{i,\mu} \begin{pmatrix} c_{E,\mu} \\ c_{P,\mu} \end{pmatrix} \exp\left[-j\omega_i t + jk_\mu(\omega_i)\mathbf{e}_{k,i}\cdot\mathbf{r}\right]. \tag{56}$$

Here $\mu = L$ or U, $|c_{E,\mu}|^2 + |c_{P,\mu}|^2 = 1$, $\mathbf{e}_{k,i}$ is the propagating direction of the ith wave, and $k_\mu(\omega_i)$ has been obtained in Eq. (29). Also, in this case, we can consider that the μ-branch excitonic polariton is the solution of the equation

$$\left[\nabla^2 + k_\mu^2(\omega_i)\right] f_{i,\mu}(\mathbf{r}) = 0. \tag{57}$$

Then we take the nonlinear interactions into account. From the preceding section, we know that when $\omega \leqslant \omega_\alpha + \Delta_{\text{LT}}$, $k_U(\omega)$ becomes imaginary, so in the strong coupling regime, where Δ_{LT} is large enough to fulfill this condition, we only need to consider the lower branch polaritons and rewrite Eq. (55) as

$$\left[\nabla^2 + k_L^2(\omega_i)\right] f_{i,L}(\omega_i, \mathbf{r}) = \chi_L^{(3)} \prod_{j\neq i} f_{j,L}. \tag{58}$$

Here the third-order nonlinear coefficient $\chi_L^{(3)} = \frac{2M}{\hbar}\frac{V_{12,34}}{{l_\alpha}^2}\prod_{j\neq i} c_{P,L}(\omega_j)$.

Besides, it has to satisfy the following conditions:

$$\begin{aligned} &\omega_1 + \omega_2 - \omega_3 - \omega_4 = 0, \\ &k_L(\omega_1)\mathbf{e}_{k_1} + k_L(\omega_2)\mathbf{e}_{k_2} - k_L(\omega_3)\mathbf{e}_{k_3} - k_L(\omega_4)\mathbf{e}_{k_4} = 0. \end{aligned} \tag{59}$$

This result is similar to four-wave interaction in nonlinear optics, so the third-order nonlinear interaction process between light waves can be applied to the excitonic polaritons. Some

experimental results have shown that the third-order nonlinear coefficient $\chi_L^{(3)}$ of an excitonic polariton is much larger than that of the light wave.

Next we consider the nonlinear interaction of the excitonic polariton in a rotational system and take the decoherence process into account. Discussed in the preceding section, in a rotational system the left-hand side of Eq. (55) has to add terms that are proportional to $\frac{|\mathbf{v}_R|}{c}$, and these terms result in the propagating constant $k_L(\omega)$ changes to $k_L(\omega)+\delta k_L(\omega)$ and $\delta k_L(\omega)=\eta_{\text{eff},L}(\omega)(\mathbf{v}_R\cdot\mathbf{e}_k)$. As for the decoherence process, we showed that when $\eta_{\text{eff},L}\ll\eta_p$, the influence of the decoherence process is that it generates an imaginary part in the propagating constant and makes it change into $k_L(\omega)+j\gamma(\omega)$ and $\gamma(\omega)\approx\eta_{\text{eff},L}\frac{\Gamma_\alpha}{2k_L(\omega)}$. Therefore, Eq. (58) becomes

$$[\nabla^2+(k_L+\Delta k_L)^2]f_{i,L}=\chi_L^{(3)}\prod_{j\neq i}f_{j,L} \tag{60}$$

and $\Delta k_L=\delta k_L+j\gamma_L\approx\eta_{\text{eff},L}\left[(\mathbf{v}_R\cdot\mathbf{e}_{k,i})+\frac{j\Gamma_\alpha}{2k_L}\right]$.

B. DFWM of microcavity excitonic polaritons

In this section, we discuss the DFWM of the lower branch of the excitonic polariton waves (Fig. 11). The sample is on the x-y plane, and the two pump waves are propagating along the y axis, while the signal wave 1 propagates along the $+x$ axis, so the idler 2 propagates in its opposite direction. We assume that the angular velocity of the system $\Omega=\Omega\mathbf{e}_z$ and the size of the interferometer is large enough that the velocity $\mathbf{v}_R$ can be approximated as an invariant vector parallel to x direction. Therefore, we have

$$\begin{aligned}
&\omega_1=\omega_2=\omega_3=\omega_4=\omega,\\
&\delta\mathbf{k}_{L,1}=\eta_{\text{eff},L}(\mathbf{v}_R\cdot\mathbf{e}_x)\mathbf{e}_x=\delta k\mathbf{e}_x,\\
&\delta\mathbf{k}_{L,2}=\eta_{\text{eff},L}[\mathbf{v}_R\cdot(-\mathbf{e}_x)](-\mathbf{e}_x)=\delta k\mathbf{e}_x,\\
&\delta\mathbf{k}_{L,3}=\delta\mathbf{k}_{L,4}=0.
\end{aligned} \tag{61}$$

Assume that the pump waves are strong enough and their amplitude variation can be neglected. Therefore, the coupling equations of the signal and idler wave can be dealt with by the slowly varying amplitude approximation,

$$\begin{aligned}
f_1(x,t)&=f_s(x)\exp(-j\omega t+jk_Lx)+\text{c.c.},\\
f_2(x,t)&=f_c(x)\exp(-j\omega t-jk_Lx)+\text{c.c.}
\end{aligned} \tag{62}$$

If we use the notations $\kappa_s=\frac{\chi^{(3)}f_3f_4}{k_L+\Delta k+j\gamma}$ and $\kappa_c=\frac{\chi^{(3)}f_3f_4}{k_L-\Delta k+j\gamma}$, the coupling wave equations become

$$\begin{aligned}
\frac{df_s}{dx}&=(j\delta k-\gamma)f_s-j\kappa_sf_c^*,\\
\frac{df_c^*}{dx}&=-(j\delta k-\gamma)f_c^*-j\kappa_c^*f_s.
\end{aligned} \tag{63}$$

The solutions of the above equations have the following form:

$$\begin{aligned}
f_s&=Ae^{jqx}+Be^{-jqx},\\
f_c&=Ce^{jqx}+De^{-jqx}.
\end{aligned} \tag{64}$$

Here

$$q=\sqrt{\kappa_s\kappa_c^*+(\delta k+j\gamma)^2} \tag{65}$$

and

$$\begin{aligned}
\kappa_s\kappa_c^*&=\frac{|\chi^{(3)}f_3f_4|^2}{{k_L}^2-\delta k^2+\gamma^2-2j\gamma\delta k}\\
&\approx\frac{|\chi^{(3)}f_3f_4|^2}{{k_L}^2-\delta k^2+\gamma^2}.
\end{aligned} \tag{66}$$

Let $\kappa^2=\frac{|\chi^{(3)}f_3f_4|^2}{{k_L}^2-\Delta k^2+\gamma^2}$, so

$$q^2=(\bar\kappa^2+\Delta k^2-\gamma^2)+2j\gamma\Delta k. \tag{67}$$

If the intensities of the pump pulse are strong enough that $\bar\kappa^2+\Delta k^2-\gamma^2>0$, then neglecting the imaginary term $\gamma\Delta k$, we get

$$q\approx\sqrt{\bar\kappa^2+\Delta k^2-\gamma^2} \tag{68}$$

as a real quantity.

Here we can obtain the coefficients A, B, C, and D by the boundary conditions of the signal and its conjugate waves. As is illustrated in Fig. 12, the boundary conditions can be expressed as

$$\begin{aligned}
f_s(0)&=F_{s,0},\\
f_c(l)&=0.
\end{aligned} \tag{69}$$

Then

$$\begin{aligned}
f_s(x)&=F_{s,0}\frac{q\cos q(l-x)+(\gamma-j\Delta k)\sin q(l-x)}{q\cos ql+(\gamma-j\Delta k)\sin ql},\\
f_c(x)&=F_{s,0}^*\frac{j\kappa^*\sin q^*(l-x)}{q^*\cos q^*l+(\gamma+j\Delta k)\sin q^*l}.
\end{aligned} \tag{70}$$

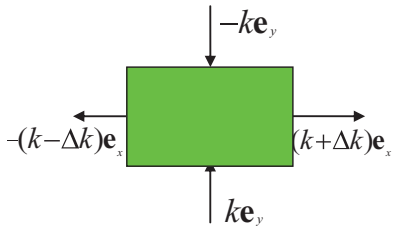

FIG. 11. (Color online) Degenerate four-wave mixing.

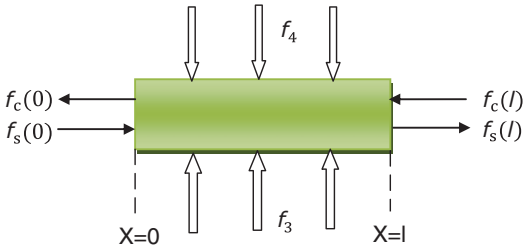

FIG. 12. (Color online) Boundary conditions.

Now we write the solutions of the coupling wave equations into the following form:

$$f_s(x) = F_{s,0}\frac{\cos[q(l-x)-\beta]}{\cos(ql-\beta)}\frac{S(x)}{S(0)}\exp[j\theta_s(0)-j\theta_s(x)],$$
$$f_c(x) = F^*_{s,0}\frac{j\kappa}{\sqrt{q^2+\gamma^2}}\frac{\sin q(l-x)}{\cos(ql-\beta)S(0)}\exp[-j\theta_s(0)]. \quad (71)$$

Here we neglect the imaginary part of q and

$$\cos\beta = \frac{q}{\sqrt{q^2+\gamma^2}},$$
$$S(x) = \sqrt{1+\left[\frac{\cos\beta}{\cos(ql-\beta)}\frac{\delta k\ \sin q(l-x)}{q}\right]^2}, \quad (72)$$
$$\theta_s(x) = \tan^{-1}\left[\frac{\cos\beta}{\cos(ql-\beta)}\frac{\delta k\ \sin q(l-x)}{q}\right].$$

If we rewrite Eq. (70) in the form

$$f_s(x) = F_s(x)\exp\{j[\theta_s(0)-\theta_s(x)]\},$$
$$f_c(x) = jF_c(x)\exp[-j\theta_s(0)], \quad (73)$$

and inset the above equation into Eq. (62), we can get the signal wave and the idler wave,

$$f_1(x,t) = 2F_s(x)\cos[\omega t - k_L x + \theta_s(x) - \theta_s(0)],$$
$$f_2(x,t) = 2F_c(x)\sin[\omega t + k_L x + \theta_s(0)]. \quad (74)$$

We can get the outgoing signal wave at $x = l$ and the idler wave exit at $x = 0$; therefore, the phase difference between the signal and the idler at the two boundaries of the medium is

$$\Delta\theta = 2\theta_s(0) - \frac{\pi}{2}, \quad (75)$$

and $\theta_s(0) = \tan^{-1}(\frac{\cos\beta}{\cos(ql-\beta)}\frac{\sin ql}{q}\delta k)$. If we take the approximation $\frac{\sin ql}{q}\delta k \approx \delta kl$, then

$$\theta_s(0) = \tan^{-1}\left(\frac{\cos\beta}{\cos(ql-\beta)}\delta kl\right)$$
$$\approx \frac{\cos\beta}{\cos(ql-\beta)}\delta kl. \quad (76)$$

So the phase difference between the outgoing signal wave at $x = l$ and the outgoing idler wave at $x = 0$ is similar to the Sagnac phase difference between two counterpropagating waves at the same interval. It can thus provide the information of the angular velocity of the system. However, we shall emphasize that the two counterpropagating waves are intrinsically coherent and so DFWM can be used to construct the hybrid interferometer.

V. CONCLUSION

In Secs. II–IV, we have presented the theoretical treatments for the Sagnac effect of the excitonic polaritons. It has been shown that the excitonic polariton wave is the coupling of the light wave and excitonic wave, so its Sagnac coefficient $\eta_{\mathrm{eff},i}$ is the function of the frequency of ω. The dependence of $\eta_{\mathrm{eff},i}$ on ω is very sensitive at the neighborhood of the resonant frequency of photon and exciton. By choosing the frequency appropriately, the excitonic polaritons wave can provide us with a large value of $\eta_{\mathrm{eff},i}$ (for example, $\approx 10^3$ times of the η_p) and a moderate photon proportion simultaneously. It is also clarified that the excitonic polaritons in the microcavity with one or a few quantum wells embedded in it are 2D quasiparticles, and the direct transitions from photons to the microcavity excitonic polaritons and its inverse process are permitted. In addition, the excitonic state can be manipulated by some methods, for example, applying external electric or magnetic field, so the value of $\eta_{\mathrm{eff},i}$ can be manipulated to bigger values. However, an intrinsical difficulty still exists that the decoherence time of the excitonic polaritons is very short, even though this time is much larger than that of bulk excitonic polaritons. As a result, we discuss the Sagnac effect of degenerate four-wave mixing of the excitonic polaritons. We find that the two counterpropagating waves, the signal wave and its conjugate wave, have a phase difference that has a form similar to the value we get from the original Sagnac effect and can thus provide the information about the angular velocity of the system. More importantly, these two waves are coherent intrinsically and so are helpful for achieving a high sensitivity. Since the polariton degenerate four-wave mixing has been measured by experiments, we believe that the Sagnac interferometer based on the excitonic polariton wave in a semiconductor microcavity is feasible.

*gulijuan0317@gmail.com

[1]M. G. Sagnac, C. R. Acad. Sci. **157**, 708 (1913).
[2]E. J. Post, Rev. Mod. Phys. **39**, 475 (1967).
[3]W. W. Chow, J. Gen-Banacloche, L. M. Pedrotti, V. E. Sander, W. Schleich, and M. O. Scully, Rev. Mod. Phys. **57**, 61 (1985).
[4]L. N. Menegozzi and W. E. Lamb, Jr., Phys. Rev. A **8**, 2103 (1973).
[5]J. E. Zimmerman and J. E. Mercereau, Phys. Rev. Lett. **14**, 887 (1965); O. Avenel, Yu. Mukharsky, and E. Varoquaux, J. Low Temp. Phys. **135**, 745 (2004).
[6]F. Hasselbach and M. Nicklaus, Phys. Rev. A **48**, 143 (1993).
[7]M. Dresden and C. N. Yang, Phys. Rev. D **20**, 1846 (1979); J. J. Sakurai, *ibid.* **21**, 2993 (1980).
[8]K. Bongs and K. Sengstock, Rev. Prog. Phys. **67**, 907 (2004).
[9]F. Zimmer and M. Fleischhauer, Phys. Rev. Lett. **92**, 253201 (2004).
[10]K. Huang, Proc. R. Soc. London **208**, 352 (1951).
[11]J. J. Hopfield, Phys. Rev. **112**, 1555 (1958); J. J. Hopfield and D. G. Thomas, *ibid.* **122**, 35 (1961).
[12]E. J. Rashba and M. G. Sturge, *Excitons* (North-Holland, New York, 1987).
[13]G. Khitrova, H. M. Gibbs, F. Jahnke, M. Kira, and S. W. Koch, Rev. Mod. Phys. **71**, 1591 (1999).
[14]Th. Ostreich, K. Schonhammer, and L. J. Sham, Phys. Rev. Lett. **74**, 4698 (1995).
[15]J. J. Baumberg and P. G. Lagoudakis, Phys. Status Solidi B **242**, 2210 (2005).

[16]P. G. Savvidis, J. J. Baumberg, R. M. Stevenson, M. S. Skolnick, D. M. Whittaker, and J. S. Roberts, Phys. Rev. Lett. **84**, 1547 (2000).
[17]M. Romanelli, C. Leyder, J. Ph. Karr, E. Giacobino, and A. Bramati, Phys. Rev. Lett. **98**, 106401 (2007).
[18]G. Messin, J. Ph. Karr, A. Baas, G. Khitrova, R. Houdre, R. P. Stanley, U. Oesterle, and E. Giacobino, Phys. Rev. Lett. **87**, 127403 (2001).
[19]M. Shirane, C. Ramkumar, Yu. P. Svirko, H. Suzuura, S. Inouye, R. Shimano, T. Someya, H. Sakaki, and M. Kuwata-Gonokami, Phys. Rev. B **58**, 7978 (1998).
[20]J. M. Blatt, K. W. Boer, and W. Brandt, Phys. Rev. **126**, 1691 (1962).
[21]L. V. Keldysh and A. N. Kozlov, Sov. Phys. JETP **27**, 521 (1967).
[22]E. Hanamura and H. Haug, Phys. Rev. **33**, 209 (1977).
[23]B. Gil, S. Clur, and O. Briot, Solid State. Commun. **104**, 267 (1997).
[24]A. V. Rodina, M. Dietrich, A. Goldner, L. Eckey, A. Hoffmann, Al. L. Efros, M. Rosen, and B. K. Meyer, Phys. Rev. B **64**, 115204 (2001).
[25]C. Weisbuch, M. Nishioka, A. Ishikawa, and Y. Arakawa, Phys. Rev. Lett. **69**, 3314 (1992); C. Weisbuch, H. Benisty, and R. Houdre, J. Lumin. **85**, 271 (2000).
[26]V. Savona, L. C. Andreani, P. Schwendimann, and A. Quattopani, Solid State. Commun. **93**, 733 (1995).
[27]M. S. Skolnick, T. A. Fisher, and D. M. Whittaker, Semicond. Sci. Technol. **13**, 645 (1998).
[28]Y. Toyozawa, Prog. Theor. Phys. Suppl. **12**, 111 (1959); U. Heim and P. Wiensner, Phys. Rev. Lett. **30**, 1205 (1973).
[29]F. Tassone, C. Piermarocchi, V. Savona, A. Quattropani, and P. Schwendimann, Phys. Rev. B **56**, 7554 (1997); F. Tassone and Y. Yamamoto, *ibid*. **59**, 10830 (1999).